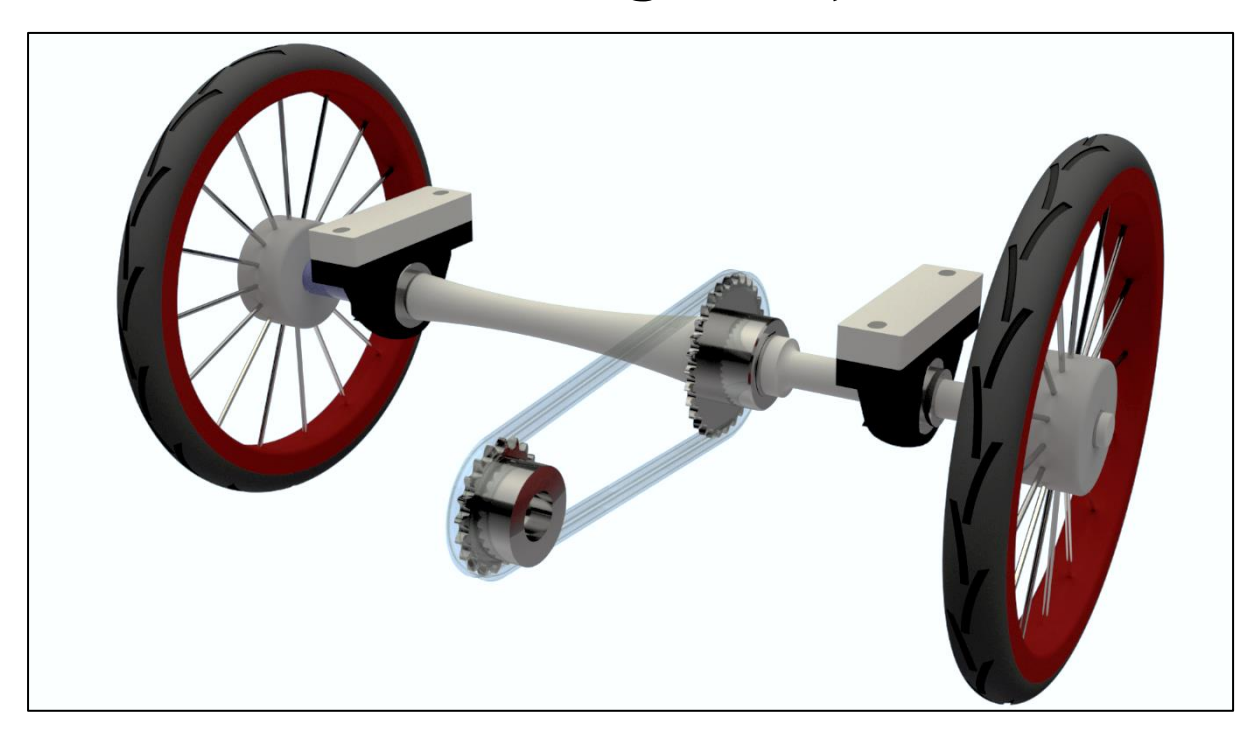
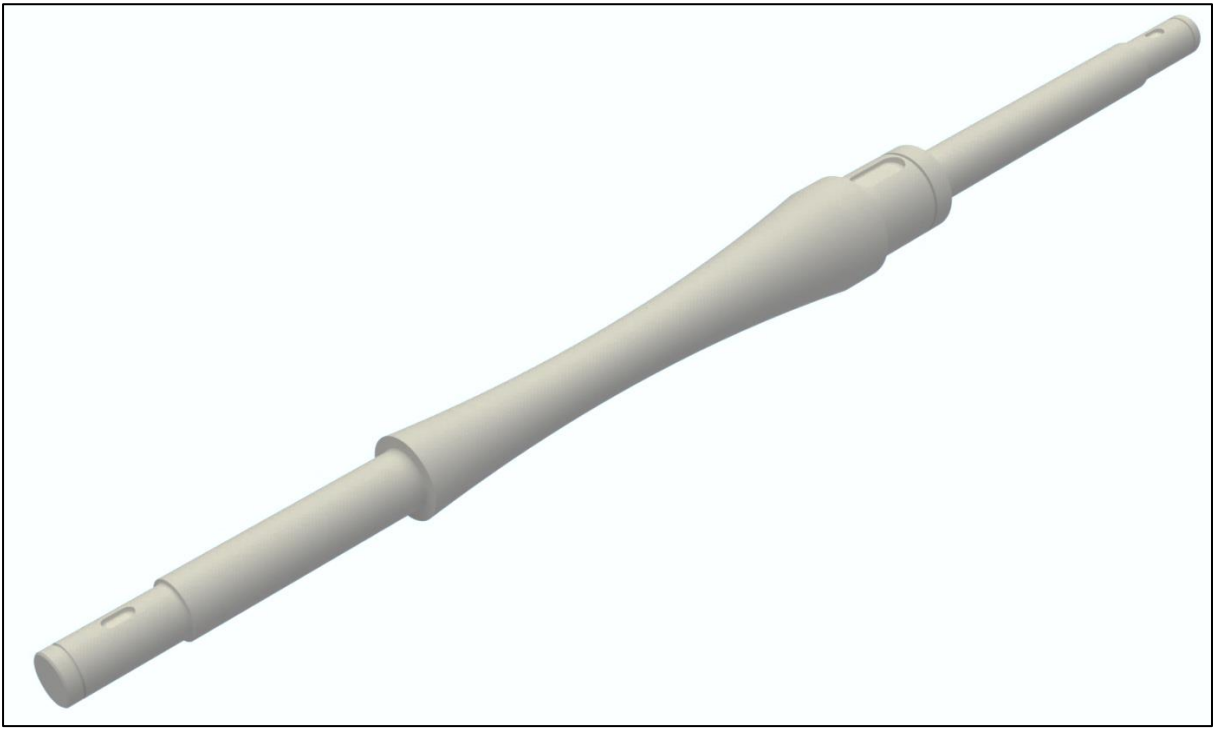
Shaft Design Project





SD-167: Harry Mills and Rodrigo Madurga

Contents

1. Summary	2
2. Design Iterations	3
3. Evaluation	9
4. References	15

1. Summary

This assignment was to design a shaft and sub-assembly for an electric trike that could withstand the forces in the system whilst adhering to a set of requirements limiting the dimensions and material choice.

Throughout the design process we considered a range of materials and designs to meet the criteria in the brief. Ultimately, we decided to use Low alloy Manganese-Molybdenum Steel as the material since it allowed a more efficient design with a lower final mass that could withstand the force present in the system. A chain drive from the motor to the shaft was used in the final design due to the cost-effectiveness, ease of maintenance and widespread availability of simplex chains making the system more maintenance friendly. Pilot-bored sprockets retained by circlips with a parallel key to transmit torque are also used as these are user-friendly (easy to assemble). We also chose pillow-block roller bearings as this was a convenient way to mount the shaft to the chassis whilst also being study enough to withstand the loading conditions of the system.

Along with fulfilling the required aspects of the shaft and sub-assembly design we also explored further ideas to optimize the shaft, such as saving weight while not increasing stress by having long tapering sections which were designed with the use of 3D modelling analysis of the stresses in the shaft geometry. Also, we investigated ways of decreasing the stresses in the shaft to optimize the shaft by saving weight and embodied carbon since lower stresses allow a smaller shaft to be used. For example, we used a spacing sleeve between the wheel and bearing rather than a circlip to axially located the bearing since circlip grooves have very high stress concentrations.

2. Design Iterations

Our initial rough concept is shown in Figure 1 below:

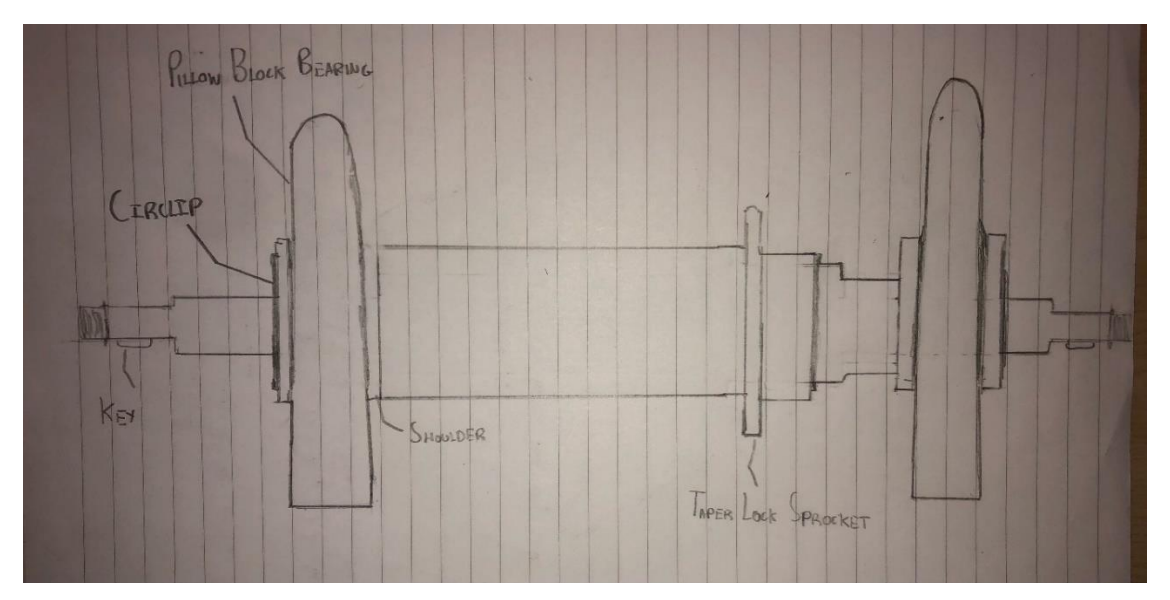


Figure 1: First shaft design concept

As pointed out in the labels, the shaft consists of a taper lock sprocket between two pillow block bearings. The bearings are fixed to the shafts by a circlip on one end and a shoulder on the other. The wheels and sprocket are fixed with the same principle, but a key is also used. Additionally, the wheels have a thread to keep them fixed axially

Iteration 1

Before performing our first iteration, we wanted to make sure we understood how the fixing mechanism of a taper lock bush works, so we did some research and asked about it in the studio sessions. After some insight on the installation of these sprockets, we decided that using this type of sprocket increased the difficulty of maintenance and assembly, since it required fixing it to a sperate hub before fixing it to the shaft itself. Figure 2 displays the arrangement of holes where the bolts would have to be oiled and threaded to fix the sprocket to the hub.

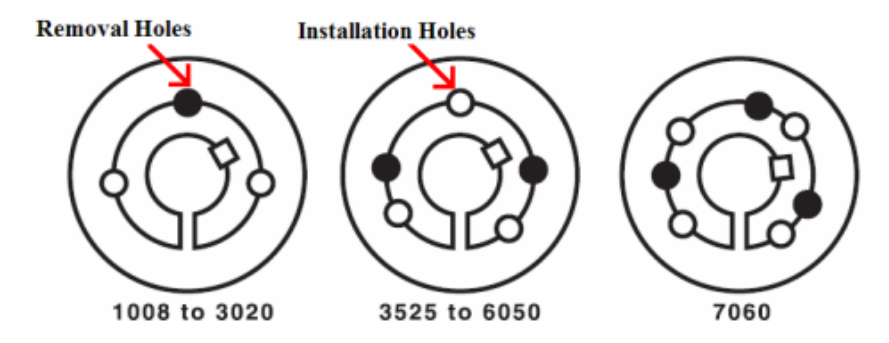


Figure 2: Taper lock Bushing installation diagrams [Gates, 2006]

ME20018 – Shaft Design SD-167

The assistant that attended us at the studio emphasized on how the whole process is very complicated and inconvenient to do. Therefore, we decided requirement 34 should be tackled in our first iteration:

'Minimise maintenance needs for the shaft sub-assembly.'

To meet this additional requirement, we thought this iteration should change the type of sprocket being used from a taper lock to a plate wheel or pilot bore sprocket. We also decided at this stage to use a chain drive going forward rather than a belt drive since chains are more common (therefore cheaper), easier to maintain (can be split without being broken) and more widely available (any local bike shop would have a replacement).

After looking into sprockets, we realised that the sprocket size of 220mm diameter we initially chose exceeded the maximum shaft centreline to chassis distance. This is illustrated in figure 3 below:

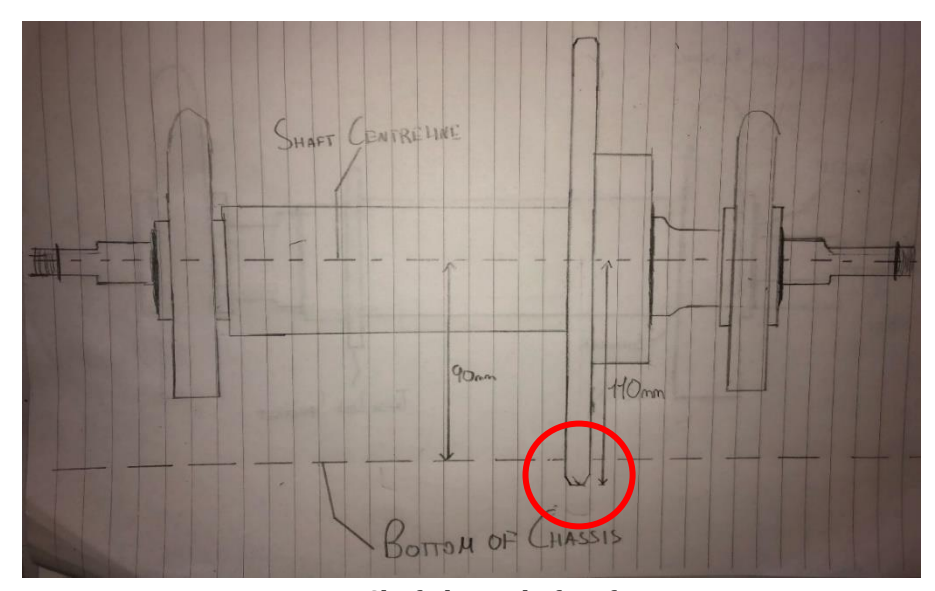


Figure 3: Shaft design before first iteration.

Hence 5 became the second requirement dealt with in this iteration:

'The shaft centreline shall be no more than 90mm from bottom of chassis'

To deal with this, the sprocket size should be reduced to a size that allows the requirement to be met, but also maintains the gear ratio calculated for the shaft to still work properly within the required parameters.

Iteration 2

At this stage of the design, we realized we did not meet the following requirement:

'While the load is misaligned, placing 75% of maximum load on one side, 25% on the other, the shaft shall not fail.'

Using the shaft generator analysis in Autodesk Inventor, we obtained the bending moments along the shaft with the weight in a 75:25 distribution at each wheel. Putting the values into our stress analysis spreadsheet, the results in Table 1 show that the shaft fails at the first bearing and sprocket.

Table 1: Stress analysis sheet showing failure at bearing and sprocket

	Symbol	Units											
Material Strength Design Factor	Sy Ny	Mpa		525 3.74									
			wheel			be	aring	sprocket			wheel		
Node: Desc.			1 Circlip	keyseat	2 shoudler	3 circlip	4 shoulder	5 shoulder	6 keyseat	7 circlip	10 shoulder	keyseat	11 Circlip
Diameter	d	mm Nm Nm	30 0 0	0	0	141	141	343 -132	343	343 -132		0 0	0
Combined BM Torque U Bending SCF Torsion SCF	M Q Km Ks	Nm	00 5 3	-32.5 2.1	-32.5 2.1	-32.5 5	-32.5 2.2	1.7	2.1	5	32.5	32.5	0 5
	D/d r/d				1,167 0.033		1.429			1.075	1.167 0.033		
Bending Stress Torsional Stress Combined Stress Allowable Stress	σ τ σ' Sy/Ny	Mpa Mpa Mpa Mpa	0.0 0.0 0.0 140.4	-18.4 18.4 140.4	-10.4 10.4 140.4	-14.7 225.1 140.4	-7.3 78.0 140.4	0.0 148.4 140.4	0.0 251.5 140.4	555.5 140.4	10.4 10.4 140.4	18.4 18.4 140.4	0.0 0.0 140.4
	201 200	5550	0%	13%	7%	160%	56%	106%	179%	396%	7%	13%	0%

To solve this, various approaches were considered. The material could be changed in to a stronger one that can support a higher stress. Also, diameter of the circlips and shoulders could be increased, as well as the dimensions of the key, to allow for a higher stress. Furthermore, the bearing and sprocket could be moved to a different point on the shaft with a lower bending moment.

In addition, we also considered adding a stress relief groove into the design. Figure 4 shows two ways in which adding a groove can be done to reduce the stress that a bearing undergoes.

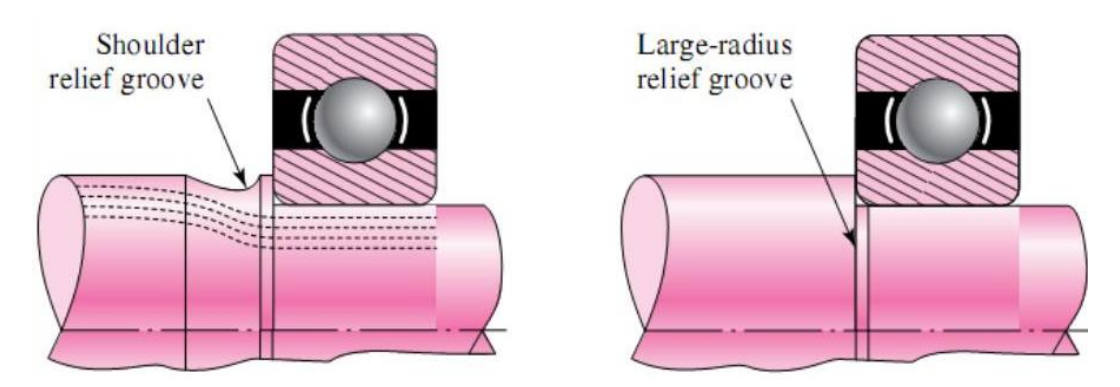


Figure 4: Shoulder and stress relief grooves for shoulders on a shaft (Dr. Aziz, 2012)

We could not find much relevant information on the effectiveness of a stress relief groove like the one shown above, so we abandoned this idea in favour of simply adjusting the shaft diameters and using the standard stress concentration factors supplied.

Iteration 3

(Replacing bearing circlip with sleeve to reduce stress, removing constraints of other bearing)

At this point both bearings on the shaft are constrained fully (with a shoulder and circlip on both). However, this is not correct as only 1 bearing needs to be constrained to allow movement for thermal expansion, as stated in requirement 16:

"The subassembly shall operate in temperatures from -10°C to 50°C"

As such, the proposed improvement initially is to remove the constraints from one of the bearings to all movement resulting from thermal expansion in the shaft.

At this point it was also decided that the remaining circlip bearing should be replaced with a spacing sleeve between the constrained bearing and the wheel. This was done to help satisfy requirements 9 and 10, which both relate to forces in the shaft not causing it to break. There was a risk of failing these requirements due to the excessive stress concentration in the circlip groove at the bearing.

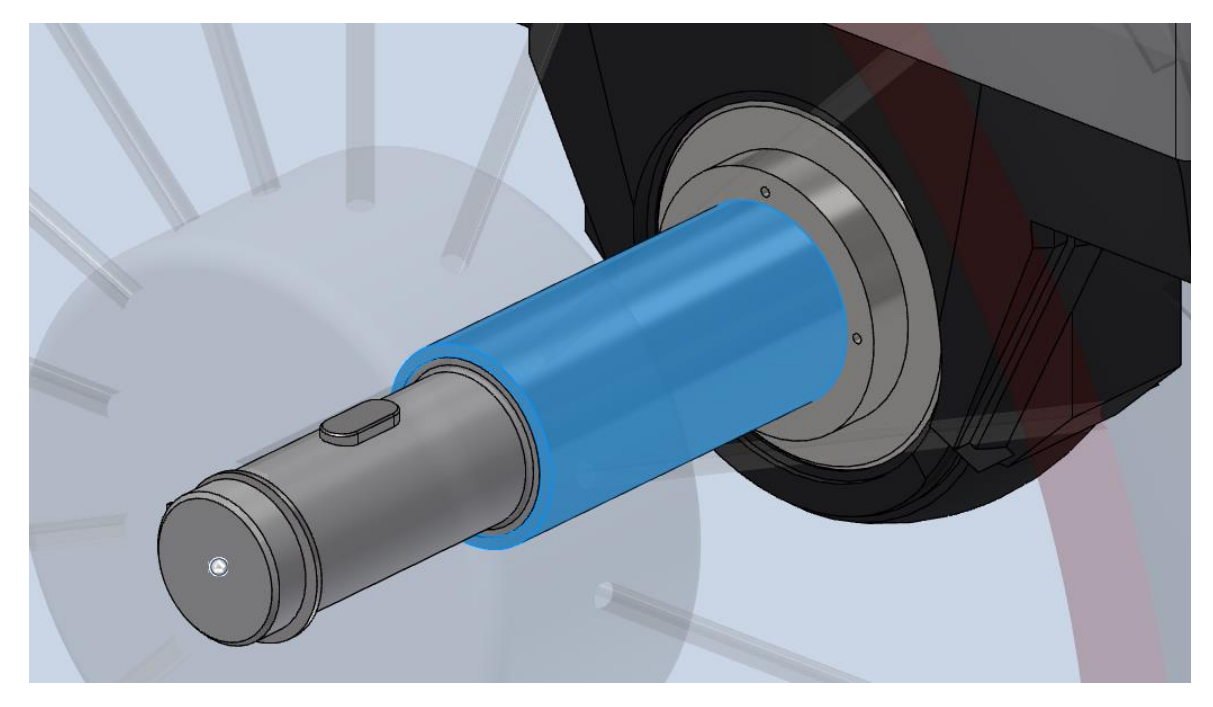


Figure 5: Example from final design of how a spacing sleeve (highlighted blue) would fit between bearing and wheel to replace a circlip

Other ways to overcome this problem would have been to increase the shaft diameter at the circlip groove (which comes at the cost of increased shaft mass/embodied carbon) or moving the position of the bearing, which we calculated would not have enough of an impact. Therefore, we decided that the most simple and effective way to satisfy the requirements would be to add a spacing sleeve between the wheel and bearing.

Iteration 4

Now that the shaft satisfied all the essential requirements, we aimed to perform one last iteration focusing on additional requirement (wish) 13:

'Minimise operational energy requirements to drive uphill by minimising mass of shaft'

We started by analyzing the design to decide which were the biggest features that could be reduced to remove excess material.

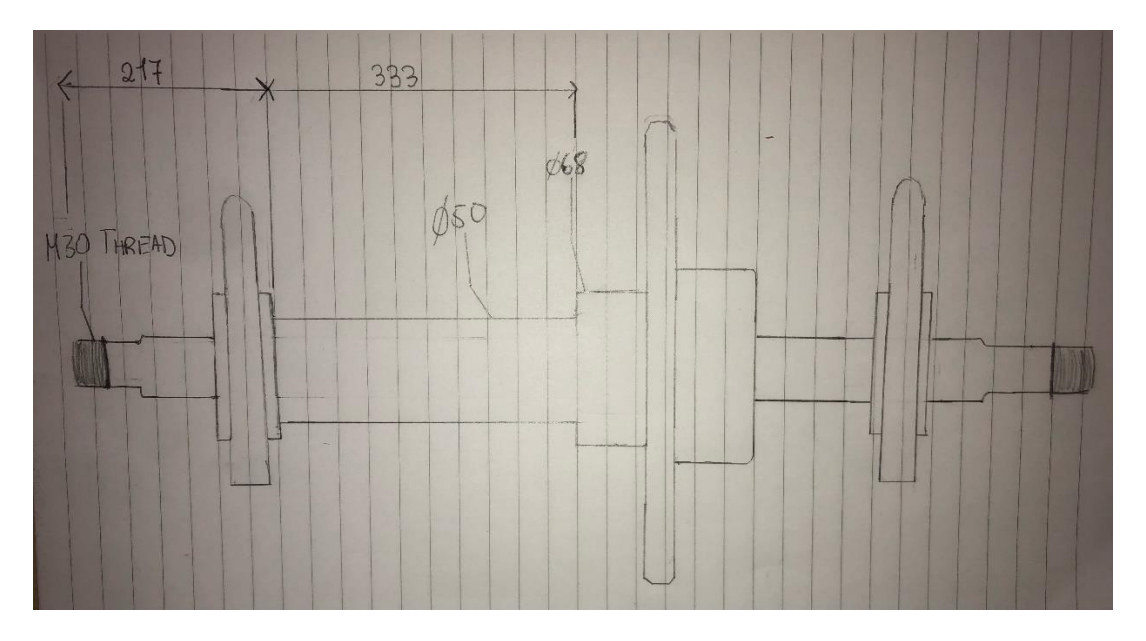


Figure 6: Sketch of design at the start of iteration 4

Figure 5 shows that on the current design, there is a 50mm shoulder for the left bearing that extends for 333mm to a 68mm shoulder for the sprocket. Using the same shaft generator analysis from iteration 2, we obtained the graph of ideal diameter shown in Figure 6 that gives the minimum diameter along the shaft that can support a bending stress of 50MPa.

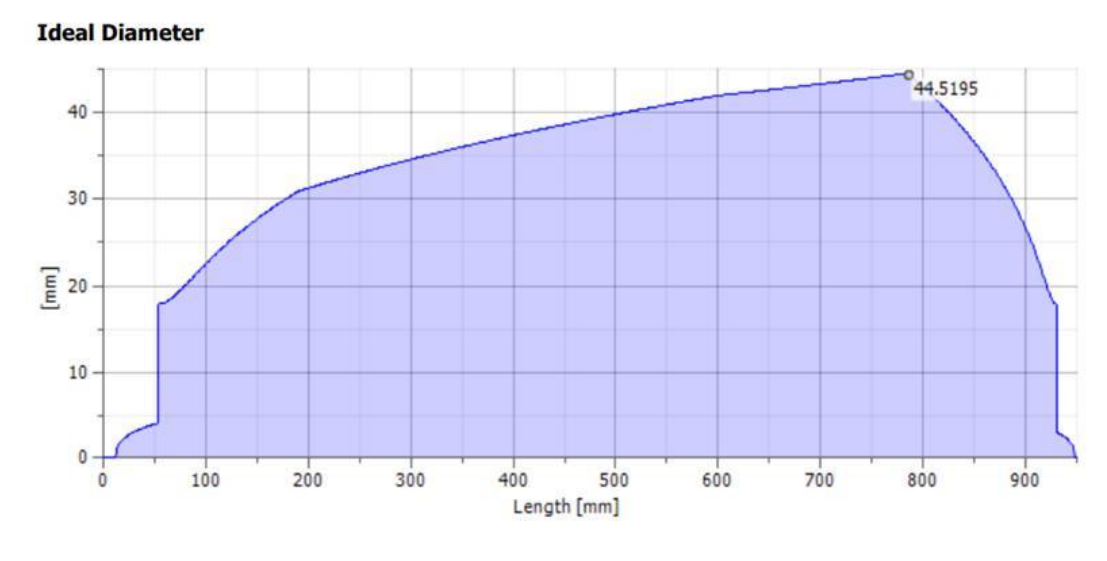


Figure 6: Graph of ideal diameter generated from Inventor Shaft Generator Analysis. This graph indicates shaft diameter to limit bending stresses to 50 MPa.

As part of this iteration, we proposed to follow the curve from 217mm to 550mm and apply it to the 333mm shoulder. Using analysis of the Inventor 3D model, we made a comparison shown in Figure 7 and 8 of the weight of the shaft before and after this change, resulting in a decrease in weight of about 5.4kg.

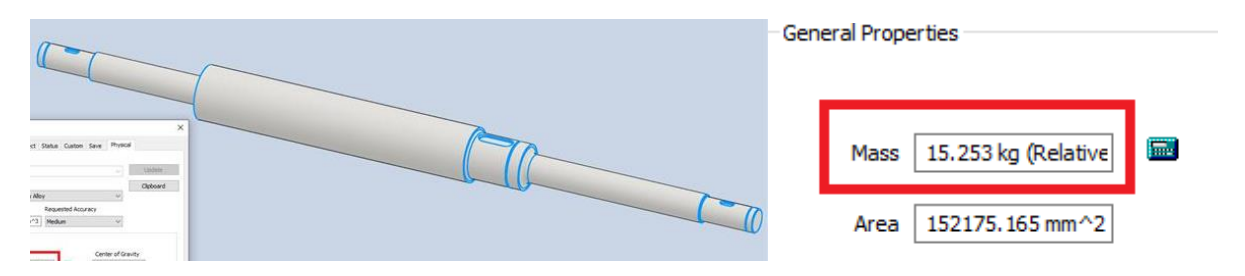


Figure 7: Shaft analysis before changing the section shape (~15.2 kg)

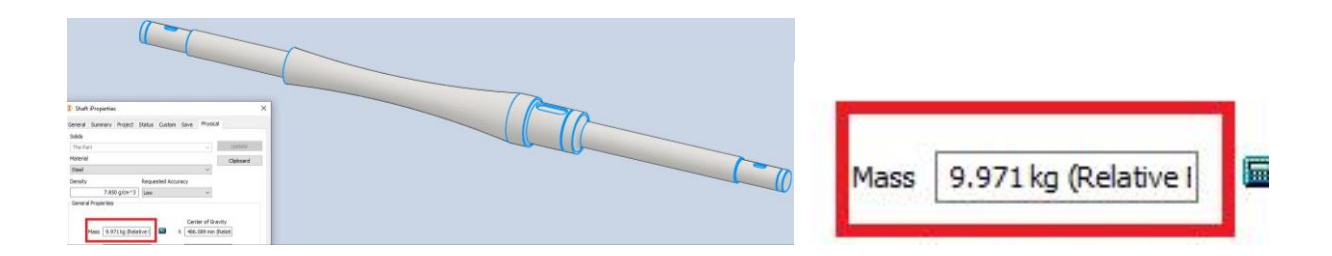


Figure 8: Shaft analysis after changing the section shape (~9.9 kg)

Additionally, we proposed to remove the threads at the end of the shaft and use a circlip to axially locate the wheels. This is instead of locking nuts or split pins that take more time to assemble and may also introduce additional machining time and part count.

3. Evaluation

3.1: Geometry:

- 1. The shaft shall position the wheel centrelines 870mm apart.
- 2. The bearings shall be located within chassis width of 670mm.
- 3. The motor sprocket/pulley shall be located within the shaded area of Figure 2.
- 4. The shaft shall be compatible with existing wheel hubs, 60mm thick, to be bored to suit shaft diameter.
- 5. The shaft centrelines shall be no more than 90mm from bottom of chassis" [Wish High]

Requirements 1, 2 and 5 are demonstrated by dimensions shown on the attached sub-assembly drawing (SD167-drawing-assembly.pdf).

Requirements 3 and 4 are not on the attached sub-assembly drawing but are evidenced below from the 3D assembly model used to generate the assembly drawing. Demonstrated below in figure 9 is that the wheel hub is 60 mm and in figure 10 that the distance from the chassis edge to motor sprocket is maximum 235 mm, to demonstrate requirements 4 and 3 respectively:

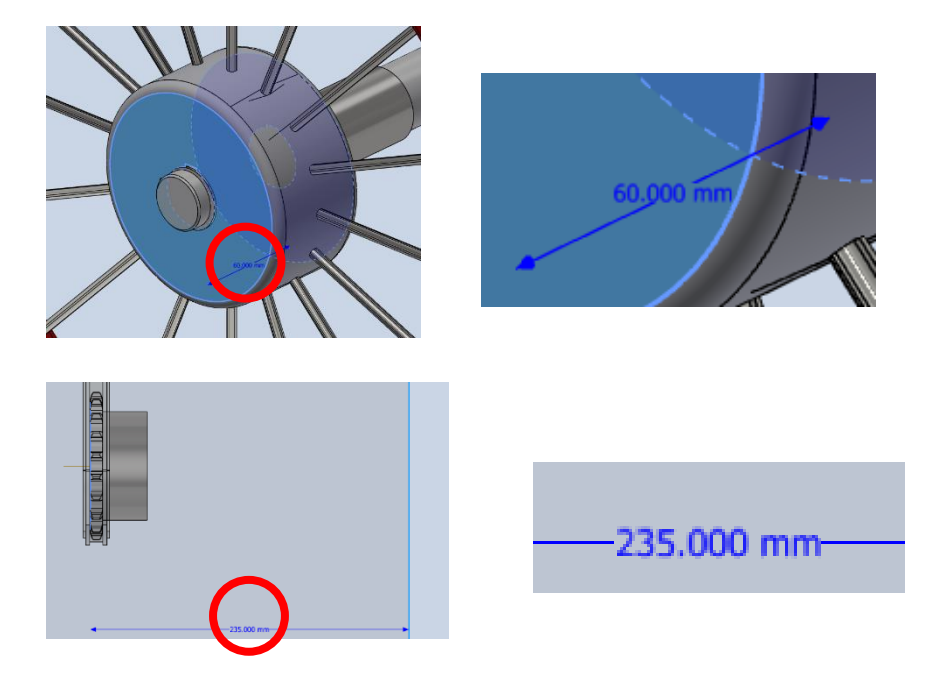


Figure 9 and 10: 3D model views with measurements of the wheel hub width and chassis to motor sprocket distance.

Therefore, we can show that the final design of our shaft fulfils all geometric requirements in the brief.

3.2 Kinematics:

- 6. Maximum vehicle speed 30 km/h
- 7. Maximum motor speed 480 rpm

Gear ratio selected = $\frac{30}{20}$ = 1.5 Radius of wheel = 0.25 mMax motor speed = 480 rpm

→
$$480 \times \frac{2\pi}{60} = 50.27 \, rad/s$$
 (1)

⇒
$$480 \times \frac{2\pi}{60} = 50.27 \, rad/s$$
 (1)
⇒ $\frac{50.27}{1.5} = 33.51 \, rad/s$ (2)
⇒ $33.51 \times 0.25 = 8.38 \, m/s$ (3)

→
$$33.51 \times 0.25 = 8.38 \, m/s$$
 (3)

$$\Rightarrow 8.38 \times \frac{60^2}{1000} = 30.16 \, km/h$$

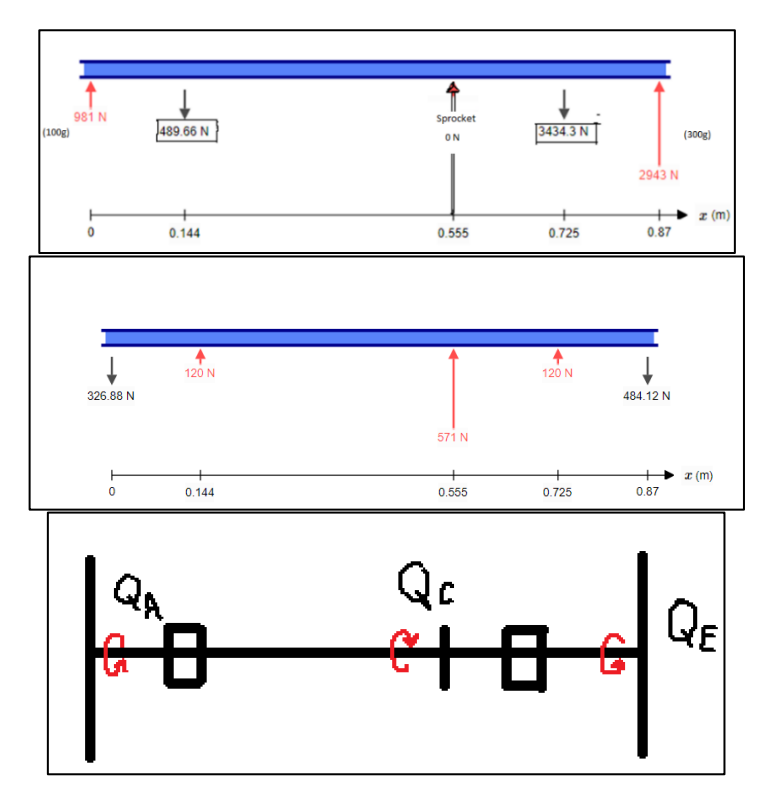
$$\Rightarrow 30.16 \times 0.95 = 28.65 \, km/h$$
(4)

→
$$30.16 \times 0.95 = 28.65 \, km/h$$
 (5)

Requirements 6 and 7 are satisfied by the calculations above. The chosen gear ratio was a 1.5 step down in speed from the motor to the shaft. As shown above this gives the maximum ideal speed (100% efficiency) as 30.16 km/h. When including a realistic efficiency estimate (95%) the estimated maximum speed is around 28.6 km/h

3.3 Forces

- 8. The shaft shall carry a maximum vertical load of 400kg across both bearings.
- 9. While the load is misaligned, placing 75% of maximum load on one side, 25% on the other, the shaft shall not fail.
- 10. While operating with max motor torque of 65 Nm at max power of 2000 W the shaft shall not fail.



Figures 11 - 13: Vertical (top), horizontal (middle) and torque (bottom) FBDs for the shaft.

The vertical FBD has been altered to account for requirement 11 so that 75% of the total weight (300 kg / 400 kg) is on the right-hand wheel. The values shown in the FBDs above were put into the calculation section of Inventor's Shaft Design Accelerator to calculate the combined bending moment easily and accurately for the specific geometry of our shaft:

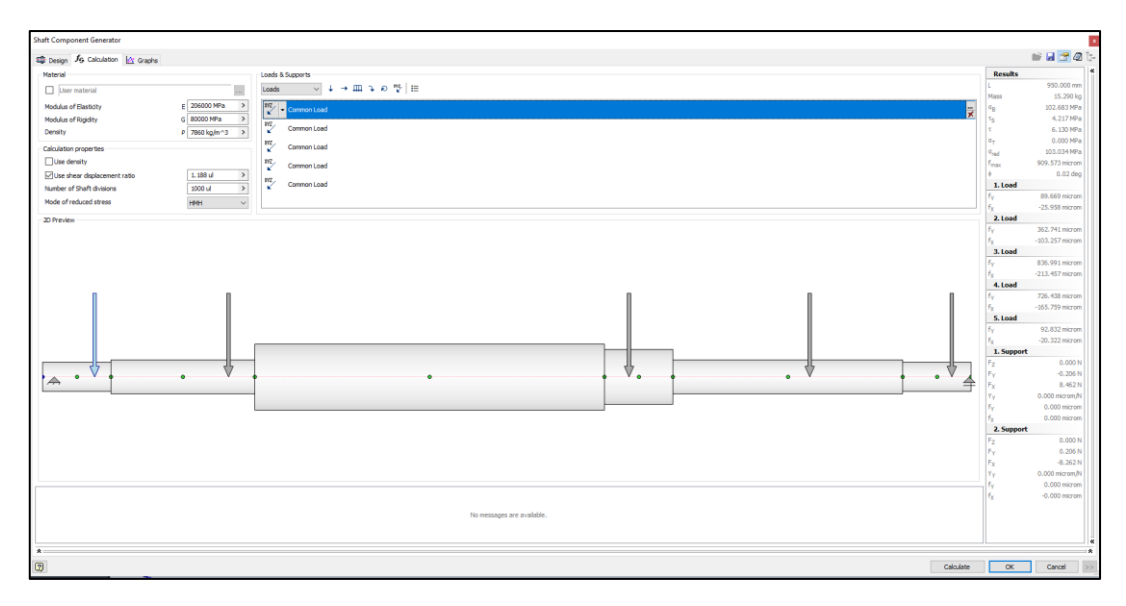


Figure 14: Inventor's Shaft Design Accelerator calculation page with corresponding loads from FBD calculations applied

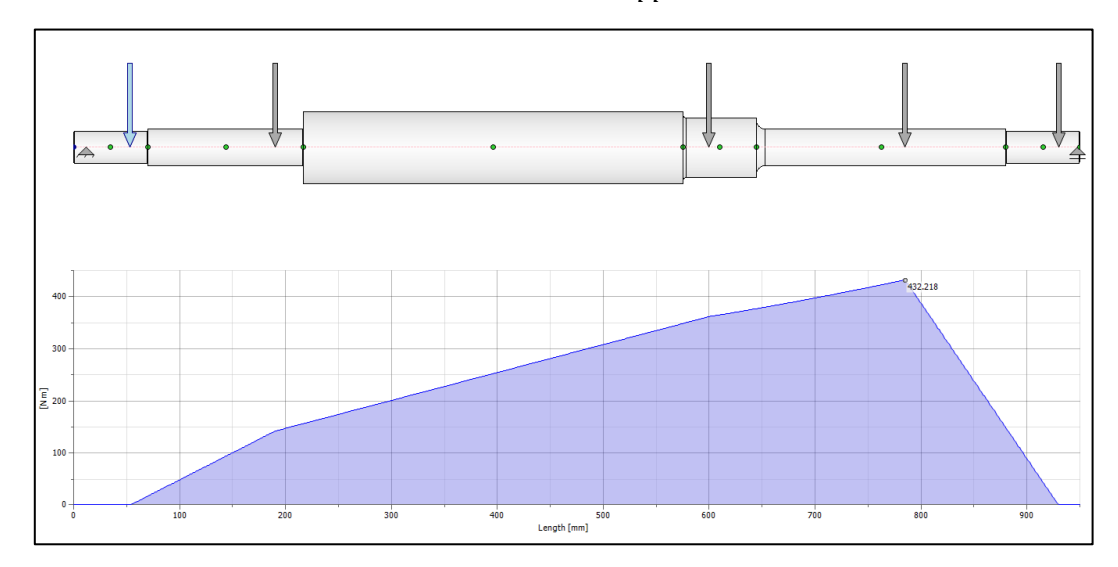


Figure 15: Combined Bending Moment graph generated by Inventor CAD analysis of the shaft geometry with corresponding loading and torque values from FBD calculations applied.

Combined bending moment values from Inventor were inputted into an excel spreadsheet to calculate the bending stresses at each node (grooves, shoulders, keyways, etc...) along the shaft. Stress concentration factors were also calculated for these nodes using the standard charts supplied. Shown below (fig. 16) is the calculation spreadsheet:

	Symbol	Units												
Material Strength	Sy	Мра	525											
Design Factor	Ny	1	3.74											
_				wheel		bearing	sprocket					wheel		
Node:			1		2	4		5	6	7		10		11
Desc.			Circlip	keyseat	shoudler	shoulder	shoulder	shoulder	keyseat	circlip	shoulder	shoulder	keyseat	Circlip
Diameter	d	mm	30	30	30	35	50	57	53.5	52.9	35	30	30	30
↑ BM		Nm	0	0	0	141	343	343	343	343	343	0	0	(
\leftrightarrow BM		Nm	0	0	0	-47	-132	-132	-132	-132	-132	0	0	(
Combined BM	М	Nm	0.0	0.0	0.0	148.6	367.5	367.5	367.5	367.5	367.5	0.0	0.0	0.0
Torque び	Q	Nm	0	-32.5	-32.5	-32.5	0	0	0	0	0	32.5	32.5	(
Bending SCF	Km		5	2.1	2.1	2.2	1.4	2.2	2.1	5	1.4	2.1	2.1	5
Torsion SCF	Ks		3	3	1.7	1.9	1.4	2	3	3	1.2	1.7	3	3
	D/d				1.167	1.429	1.360	1.193		1.075	1.629	1.167		
	r/d				0.033	0.029	0.160	0.053			0.22857	0.033		
Bending Stress	σ	Mpa	0.0	0.0	0.0	77.7	41.9	44.5	51.3	126.4	122.2	0.0	0.0	0.0
Torsional Stress	τ	Мра	0.0	-18.4	-10.4	-7.3	0.0	0.0	0.0	0.0	0.0	10.4	18.4	0.0
Combined Stress	σ'	Мра	0.0	18.4	10.4	78.0	41.9	44.5	51.3	126.4	122.2	10.4	18.4	0.0
Allowable Stress	Sy/Ny	Мра	140	140	140	140	140	140	140	140	140	140	140	140
			0%	13%	7%	56%	30%	32%	37%	90%	87%	7%	13%	0%
all <100% ?	yes													

Figure 16: Excel shaft stress calculation spreadsheet for final shaft design.

The figure above shows that at the loading conditions stated by requirements 9 - 11 the shaft will not fail even when factoring in for stress concentrations at nodes and applying a design factor.

The design factor N_y (3.74) was chosen by considering a fatigue factor b, shock factor c and safety *factor d*. The following equation was applied:

$$N_{v} = bcd ag{6}$$

We chose a fatigue factor b of 1 since the stress in the shaft varies in magnitude, but not direction.

For shock factor *c* we selected 2 since the load on the bike may be applied suddenly, rather than gradually, if the bike goes into a pothole or runs over a curb.

Lastly, to estimate a safety factor we used Pugsley's method and considered probability and seriousness of failure. For materials, workmanship, inspection and manufacture we chose 'very good' since the shaft is suitable for small-batch production. For loading and control over use we chose 'fair' as there is not much control of how the shafts responds to load over time. For quality of assessment of strength and analysis methods we chose 'good' since, as demonstrated on Figure 16, we performed a thorough analysis with stress calculations, but we could we did not account for all uncertainties. We chose the economic consequences to be 'serious' as bike repairing can be costly and danger to people to be 'not serious' since a bike accident does not have the same repercussions as with other vehicles.

Overall, these choices resulted in a safety factor of 1.7.

11. Auxiliary components (keys, clips, hubs etc) shall be sized to avoid failure.

This requirement was fulfilled using Inventor's in-built Design Accelerator calculator. Keys are used in the final design to transmit torque between both wheels and the shaft along with from the sprocket to the shaft. When placing the key and keyway the torque and shaft diameter at that point was specified and the correctly sized keyway was placed; see figures 15 and 16 below:

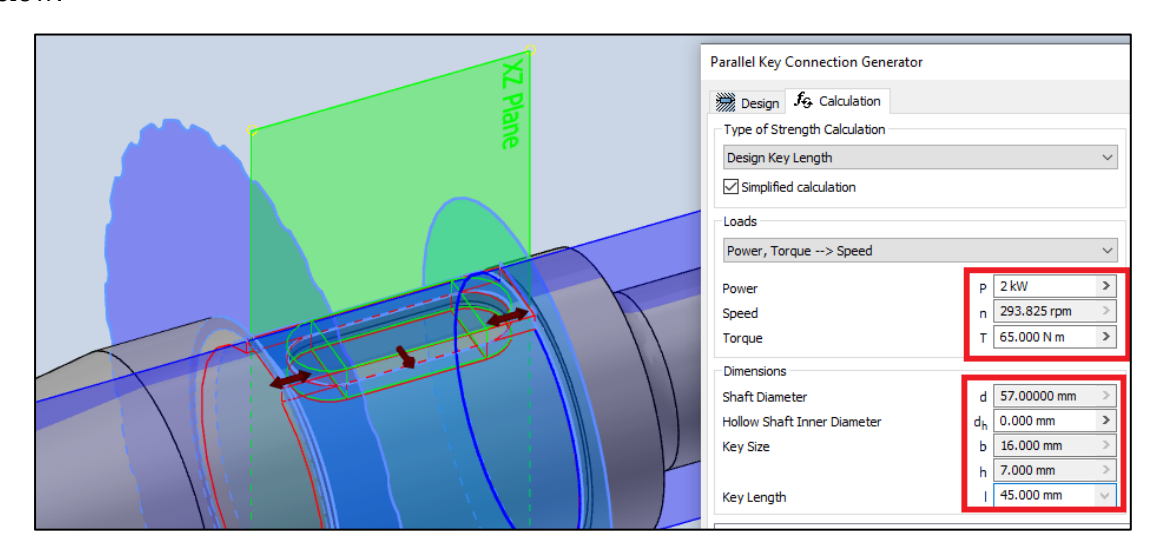


Figure 17: Placing sprocket key on the shaft with corresponding torque, power and shaft diameter shown (right)

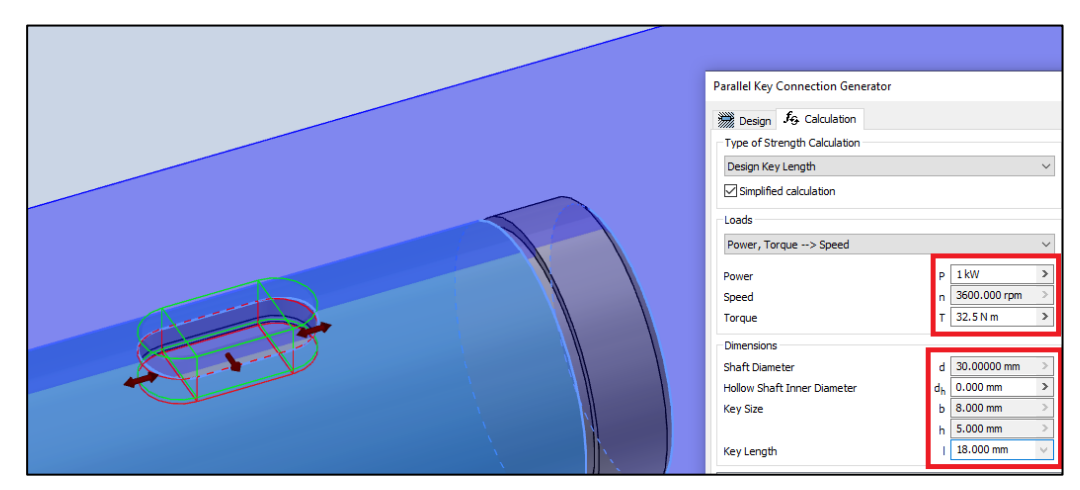


Figure 18: Placing sprocket key on the shaft with corresponding torque, power and shaft diameter shown (right)

The bearings used in the final design are SKF SYNT 35 FTF [3]. Shown below are some of the relevant force ratings used to confirm that these bearings are strong enough for use in this system:

Basic dynamic load rating	С	86.5 kN	BRE	AKING LOAI	OS
Basic static load rating	C ₀	85 kN	P _{0°}	150 kN	Breaking load
Fatigue load limit	P _u	9.3 kN	P _{55°}	250 kN	Breaking load
Limiting speed		2 050 r/min	P _{90°}	150 kN	Breaking load
Figure 19: Bearing load i	P _{120°}	95 kN	Breaking load		
rigure 19. Dearing load i	utiligs (SKI)		P _{150°}	85 kN	Breaking load
			P _{180°}	105 kN	Breaking load

ME20018 – Shaft Design SD-167

As shown in figure 17 the bearing load ratings are much higher than any of the forces considered in the FBD calculations. As a result, we decided that these bearings were acceptable for the final design.

12. Minimise operational energy requirements due to frictional losses in transfer of power [Wish – Medium]

A chain drive was chosen for the system as it has very high efficiency (even higher than a belt drive). The use of high-quality roller bearings also reduces the friction and allows higher efficiency for the whole system.

13. Minimise operational energy requirements to drive uphill by minimising mass of shaft [Wish – High]

This requirement we focused on in iteration 4 (page 7 – 8). By optimizing the diameter of the shaft in a long section which otherwise would have been a large, continued shoulder we were able to save around 5.5 kg (see details in iteration 4 section). The final mass of the shaft was 9.9 kg (assuming $\rho = 7.8 \text{ g/cm}^3$).

3.4 Materials

14. The shaft shall be made of one of the available materials given in Table 4

We chose Low alloy Manganese-Molybdenum Steel (EN16 605M36) from the table as our material.

3.5 Environment

16. The subassembly shall operate in temperatures from -10°C to 50°C

Thermal expansion in the shaft was accounted for (see also iteration 3) by having one bearing fully constrained whilst the other had no constrained applied to allow any movement resulting from changes in temperature.

3.6 Production

21. The shaft shall be suitable for small-batch production (< 50 per year)

All shafts will be produced by turning on a lathe. Due to the complex curve of the middle section (iteration 4) it may be necessary to use a CNC lathe. This is a drawback since it will potentially increase tooling cost. However, it may be beneficial since the quality of the shafts will likely be higher. We deemed this trade off acceptable since it is a relatively small batch production.

22. The transmission shall use a chain drive, V-belt drive, or synchronous belt drive.

Our shaft uses a chain drive with pilot bored sprockets.

3.7 Assembly

26. The shaft geometry shall be such that all components can be assembled from the ends of the shaft.

This is visible on the assembly drawing attached with this document.

3.7 Operation

29. The system shall operate for 10 years at full duty operation of 8h/day, 365 day/year.

Using the Fenner Transmission Selection Guide, we selected a chain drive with the following characteristics:

Service Factor: 1.1 Design Power=2.2kW Chain Pitch: 10B Power rating: 4.55

3.8 Maintenance

34. Minimise maintenance needs for the shaft sub-assembly

We opted for a pilot bore sprocket which, as opposed to a taper lock sprocket, can be fixed into the shaft simply with the use of a shoulder, circlip, and a key. Taper lock sprockets require a slightly more complicated fixing process with a separate hub that would also need components like bolts which make the whole assembly a more burdensome process and increases the total sub-assembly part count.

We also chose to use to chain drive in this instance as chain drives are more maintainable than belt drives. Chains are cheaper, more readily available, and more efficient than belt drives. For example, a chain could likely be replaced by a user at home or very easily at a local bike shop – whereas a belt drive would likely have to be ordered from a specialist supplier and would likely take longer to repair – increasing the downtime of the system.

4. References

[1] Gates Corporation, 2006. Product Application Notes, Volume 53, No.8 Available from: https://dpk3n3gg92jwt.cloudfront.net/domains/bbman2/bushinginstallation.pdf [Accessed on 1st November 2021]

[2] Dr. Aziz B.K, 2012. University of Petroleum & Minerals Mechanical Engineering Department. Chapter 18. Available from: https://www.slideserve.com/ronat/shafts-and-axles [Accessed on 1st November 2021]

[3] SKF [Online] Available from: https://www.skf.com/group/products/mounted-bearings/roller-bearing-units/pillow-block-units/productid-SYNT%2035%20FTF [Accessed on 1st November 2021]